MASTER

GPS aided adaptive complementary filter for yaw estimation under magnetic field distortion with application to quadcopters

Ilisu, H.H.

Award date:
2019

GPS aided adaptive complementary filter for yaw estimation under magnetic field distortion with application to quadcopters

CST 2019.083

H.H.Ilisu BSc. 0852221

Committee:

dr.ir.	T. Hofman	(chairman)
dr. ir.	D.J. Antunes	(thesis supervisor)
dr. ir.	A. Saccon	
ir.	N.N. Vo	(advisor)

EINDHOVEN UNIVERSITY OF TECHNOLOGY
DEPARTMENT OF MECHANICAL ENGINEERING
CONTROL SYSTEMS TECHNOLOGY

OCTOBER 22, 2019

Acknowledgment

First of all, I would like to thank dr. Duarte Antunes for his guidance and support during the project. With his patience and critical approach to my ideas, I have learned a lot in terms of research and developed myself professionally. We get to learn a lot on critical and analytic thinking, but this project was a great opportunity for me to further develop these skills with the guidance of my supervisor.

Second, I would like to thank Nam Vo from ALTEN Netherlands B.V. for his guidance on how to manage such a project with time restrictions and communication. Also a big thanks to the colleagues and managers at ALTEN Netherlands who have supported me throughout my work.

At last, I would like to thank my family and especially my wife for her mental support and caring. With this work, we close a chapter of studying and start a new chapter towards a career as a professional engineer. Throughout the years at the University of Technology Eindhoven, I have met a lot of new people with some of them becoming very close friends. I have learned a lot and now I am ready to apply my knowledge in the real world.

GPS aided adaptive complementary filter for yaw estimation under magnetic field distortion with application to quadcopters

[1]H.H.Ilisu and Duarte J. Antunes

Abstract— **This thesis addresses the problem of estimating the yaw angle of a rigid body, and it is especially intended for quadcopter applications with small pitch and roll requirements. While this is typically achieved using on-board magnetometer and gyroscope measurements, the corresponding estimates are often corrupted by magnetic field distortion. Based on a global positioning system, we show that one can still infer the yaw angle from a time-varying Kalman filter (KF-GPS), but not for all rigid body trajectories. This motivates our adaptive approach where the measurements are incorporated in a complementary filter (KF-ACF) based on confidence levels. For the magnetometer, this confidence level is based on the distance between the measurements obtained when using only the magnetometer and only the gyroscope; for the global positioning measurements, it is based on the degree of observability of the Kalman Filter model. While the main focus in on estimating the yaw angle, the adaptive complementary filter is also derived on the special orthogonal group of rotation matrices which provides the full attitude based also on accelerometer measurements. The effectiveness of the KF-ACF for yaw estimation is demonstrated by simulation results.**

I. INTRODUCTION

In recent years, quadcopters have sparkled the interest of researchers due to their challenging non linear and coupled dynamics and their impact in numerous applications. The attitude of the quadcopter is typically described by three angles: roll, pitch and yaw angle, which represent rotations around the x,y and z body fixed axis, respectively, where the z axis is aligned with the gravity vector at hover. Roll and pitch estimates are determined by the Inertial Measurement Unit (IMU) and are highly reliable for everyday use and even for autonomous flight. The estimation of yaw, denoted by ψ, however, is in many environments, subject to noises and distortions in sensors which makes obtaining a proper yaw estimation a challenging task. For example, quadcopters equipped with cameras gathering data from metal structures such as bridges or wind turbines are subject to fluctuations in the magnetic field due to the proximity to metal structures. In fact, the magnetometer sensor is highly sensitive to metal, hard- and soft iron, charged wires and actuators, and this is the main issue for yaw estimation [1], [2], [3]. When flying with an operator, these errors can be corrected manually, but when flying autonomously these can cause undesired behaviour. In fact, obtaining a correct yaw- estimation is of great importance for autonomous quadcopters. Due to their coupled dynamics, errors in angles result directly in errors in position which has an impact on the flight quality. For example, in the mentioned data acquisition setting, these errors result in blurred or poor quality images. [1]

In the literature, the problem of yaw estimation has been divided into two subcategories: the vision based attitude estimation and the non-vision based estimation. In [5], [6], [7], [8], [9], we can find attitude estimation methods based on cameras. In [5], an omnidirectional camera has been used for attitude estimation. The main algorithm for yaw estimation relies on horizon detection. A reference frame within a horizon is taken and relative rotations with respect to this horizon reconstructs the yaw angle. The advantage of this method is its robustness against different heights and weather conditions. A disadvantage of the addition of a camera is delay and latency issues in control which effected overall performance. In [6], [7], [8] we can find methods with downward looking cameras and detection of known objects for attitude estimation. The advantage of these methods is the low complexity of implementation and high accuracy. Angle estimation with a Root Mean Squared Error (RMSE) of 1.4 degrees are possible. However, the disadvantage of this method is the constraint of object detection. If the camera can not detect the known object, the ψ-angle can not be estimated. In [7], this is solved by fusing the camera with the gyroscope integration. However, the gyroscope integration results in a drift of the true angle. These methods are also highly invasive. To be able to implement them, the environment should be redesigned in order for the quadcopter to fly in it. In [9], we can see a review based on different vision based methods. We can conclude from this work that omnidirectional cameras are constrained due to their environment since horizon detection depends on outdoor environment. The constraint for downward looking cameras is thus the image quality and the highly invasiveness of the object detection.

*This work was supported by Alten Netherlands

[1]Hasan Ilisu and Duarte Antunes are with the Control Systems Technology group, Mechanical Engineering, at Eindhoven University of Technology, The Netherlands. Email: h.h.ilisu@student.tue.nl, d.antunes@tue.nl

[1]Another example with much severe consequences was the Varig Airlines flight 254, which departed from Sao Paulo and Due to a huge navigational error in which the crew entered wrong heading for the airplane, the plane diverted from the original plan and crashed, killing 13 people [4].

Non-vision based methods have been widely researched in [1], [2], [3], [10], [11], [12], [13], [14]. In [3], [10], a Multiple Magnetometer Platform (MMP) has been developed and integrated. The MMP is a platform in which a set of twelve triads of magnetometers are placed such that directional distortions are compensated. The advantage of this method is accuracy improvement by a factor four with respect to a single triad of magnetometers. The disadvantage is the requirement of a total of twelve magnetometers as addition to the metrology of the quadcopter. This method is therefore highly invasive. In [1], a first approach on using convex optimization for distortion attenuation has been proposed. This method gives a clear description of the detection of dynamic distortion. Many researchers have based their distortion detection algorithm based on stationary effects [11], [2]. This method also discusses an adaptation logic based on magnetic distortions. This idea of an adaptation logic has been proposed in [13]. Here, distortions in vector measurements such as the accelerometer and the magnetometer are handled by proposing an adaptive complementary filter. The complementary filter with fixed gain has been proposed in [12]. This method does not handle distortions in vector measurements while [13] with an adaptation logic based on similarity properties does so. However, [13] has only been tested in simulation and only on the pitch angle. One of the most interesting aspects of [13], [12] is the addition of an observer design for the complete rotation matrix. Another non-vision based method for attitude estimation is the use of a Kalman Filter for state estimation together with position sensors. In [14], this has been done for an Inertial Navigation System (INS) aided by a global positioning system (GPS). An advantage of this method is that since it follows an optimal control approach for state estimation, it is optimal in a well-defined sense. A disadvantage if that observability, required by the Kalman Filter, is not assured for every state trajectories and extra positioning sensors are required.

In this thesis, we start by proposing a method for yaw estimation based on accelerometer, gyroscope and GPS measurements (i.e., no magnetometer) and a time-varying Kalman. Hereafter, we will refer this method as KF-GPS. However, due to lack of observability such a filter does not provide an accurate yaw estimate for every state trajectory (e.g. when hovering with a fixed yaw angle, it is not possible to obtain the yaw angle from the mentioned measurements). Therefore, we propose to use the Degree of Observability (DoO) of the model used by the Kalman filter as a confidence level for the estimate obtained by this method. A confidence level is also defined for the measurement obtained from the raw magnetometer data based on the magnetic field distortion. The estimates provided by the KF-GPS and the raw magnetometer data and their confidence levels are used in an adaptive complementary filter. In spirit of [13], relying on magnetometer and gyroscope data in an adaptive manner which will be referred to as m-ACF. The rationale behind the proposed filter is that the estimate should rely on a combination between the raw magnetometer estimate and the KF-GPS estimation method. When the DoO is low, the filter should rely on the raw magnetometer measurements. Otherwise, the filter should rely on KF-GPS. In case the magnetometer measurements are distorted, the filter should shut off the magnetometer completely. This means that the confidence level condition is not met and certain disturbances distort the measurements. Hereby, with the use of the similarity property, the filter will weigh between the Kalman Filter estimation and the gyroscope integration. We will refer to this filter as the KF-ACF in which the KF-GPS, the adaptive complementary filter and the confidence levels are implemented. As an extension to this method, we propose an adaptive method for decoupled rotation matrix estimation in Special Orthogonal Group $SO(3)$ as derived in [12]. In particular, we extend the Explicit Complementary Filter (ECF) in [12] by proposing an adaptive gain instead of a fixed gain for decoupled vector measurements.

The contribution of this thesis is therefore fourfold. First we design a linear time-varying Kalman Filter for yaw estimation for Quadcopters based on accelerometer, gyroscope and GPS measurements. Second, we propose metrics to understand when measurements from the standard magnetometer based method and the KF-GPS based method are reliable or not. Third, we propose an adaptive complementary filter to cope with time-varying disturbances. Fourth, we extend the Explicit Complementary Filter (ECF) in [12] by proposing an adaptive logic such that distortions in vector measurements are handled for estimation of the rotation matrix.

The body of this thesis consists of four sections followed by conclusions and future work. In section II we provide background information and motivation for the study in which we build up towards the methodology. In section III we start with deriving an LTV Kalman Filter for yaw estimation. Here we also analyze observability and give a metric for Degree of Observability (DoO). In section IV, we define and describe the proposed adaptive logic for the complementary filter where we use the Kalman Filter as the estimator and the DoO and the similarity condition as the adaptation distortion detection measure. We then describe our vision and define an adaptation logic for the complete rotation matrix in the Special Orthogonal Group $SO(3)$ where we extend the conventional method of a static gain complementary filter to an adaptive complementary filter. In Section V, we give the simulation results of the of the KF-ACF method. After this section, conclusions and future work follow.

II. BACKGROUND AND MOTIVATION

In Section II-A, we will present the notations and assumptions which hold throughout the thesis. In Section II-B, a dynamic model of the Quadcopter will be presented from where we take the step to Section II-C in which we discuss the role of ψ-estimation. In Section II-D we will discuss the sensors which are used for attitude estimation in Quadcopter. From here, we discuss the complementary filter sensor fusion algorithm in Section II-E. Since we will be using a linear time varying Kalman filter, in Section II-F we discuss the algorithm behind the Kalman Filter. At last, in Section II-G, we describe the motivation for this study.

A. Notations and Assumptions

Throughout this thesis, the following notations and assumptions will be considered:

- The unit axes of the Body-Fixed-Frame $\{B\}$ are denoted as $[b_1, b_2, b_3]$
- The unit axis of the Inertial-Frame $\{I\}$ are denoted as $[e_1, e_2, e_3]$
- The Body-Fixed-Frame coincides with the Center of Gravity (CoG)
- The Quadcopter is assumed to be symmetric in the $[x, y]$-plane
- Aerodynamic phenomena like blade flapping are not taken into account
- Aerodynamic disturbances like wind gusts are not taken into account.

B. Quadcopter Modelling

Consider the model of a Quadcopter [15], [16]:

$$\dot{p} = v, \tag{1a}$$

$$m\dot{v} = \begin{bmatrix} 0 \\ 0 \\ mg \end{bmatrix} + R \begin{bmatrix} 0 \\ 0 \\ -F_T \end{bmatrix}, \tag{1b}$$

$$\dot{R} = RS(\Omega), \tag{1c}$$

$$I\dot{\Omega} = \tau - \Omega \times (I\Omega) \tag{1d}$$

where $p = [x, y, z]^\intercal \in \mathbb{R}^3$ and $v = [v_x, v_y, v_z]^\intercal \in \mathbb{R}^3$ denote the position and velocity respectively, represented in the $\{I\}$ frame. $m \in \mathbb{R}$ is the mass and $g \in \mathbb{R}$ is the acceleration due to gravity, $I \in \mathbb{R}^{3\times3}$ is the inertia matrix, $\tau \in \mathbb{R}^3$ is the torque input, $\Omega \in \mathbb{R}^{3\times1}$ is the angular velocity. The attitude of the quadcopter is given by a 3×3 rotation matrix which describes a rotation of coordinates expressed in Body-Fixed-Frame $\{B\}$ to coordinates expressed in the Inertial-Frame $\{I\}$. The rotation matrix can be parametrised by the Tait-Bryan rotation convention [15]:

$$R = R_z(\psi)R_y(\theta)R_x(\phi) \in SO(3), \tag{2}$$

where $[\phi, \theta, \psi]^\intercal \in \mathbb{R}^3$ are the roll, pitch and yaw angles respectively. We describe

$$S(\Omega) = \begin{bmatrix} 0 & -\Omega_z & \Omega_y \\ \Omega_z & 0 & -\Omega_x \\ -\Omega_y & \Omega_x & 0 \end{bmatrix}, \tag{3}$$

in which $S(\Omega)$ is a skew-symmetric matrix such that $S(\Omega)v = \Omega \times v$ where $\times$ denotes the vector cross product and any vector $v \in \mathbb{R}^3$.

C. The role of ψ-estimation

If we let

$$\bar{a} = \begin{bmatrix} \bar{a}_x \\ \bar{a}_y \end{bmatrix} = \underbrace{\begin{bmatrix} 1 & 0 & 0 \\ 0 & 1 & 0 \end{bmatrix}}_{D} R_y(\theta)R_x(\phi) \begin{bmatrix} 0 \\ 0 \\ T \end{bmatrix}, \tag{4}$$

where $D \in \mathbb{R}^{2\times3}$ is a projection matrix such that we only take the $[x, y]^\intercal$ components in 2D into account. $\bar{a} \in \mathbb{R}^2$ represent the accelerations in x and y is a frame which coincides with the Inertial Frame, except for a rotation in ψ. Now we can write the velocity and acceleration subsystem with respect to $\{I\}$ as:

$$\begin{bmatrix} \dot{p_x} \\ \dot{p_y} \end{bmatrix} = \begin{bmatrix} v_x \\ v_y \end{bmatrix} \tag{5a}$$

$$\begin{bmatrix} \dot{v}_x \\ \dot{v}_y \end{bmatrix} = \underbrace{\begin{bmatrix} c_\psi & -s_\psi \\ s_\psi & c_\psi \end{bmatrix}}_{R_z(\psi)} \begin{bmatrix} \bar{a}_x \\ \bar{a}_y \end{bmatrix}, \tag{5b}$$

where c_ψ and s_ψ are defined as $\cos(\psi)$ and $\sin(\psi)$ respectively and $R_z(\psi)$ is the rotation matrix to express the accelerations from $\{B\}$ in $\{I\}$.

In order to illustrate the importance of properly estimating the ψ angle a few observations about the controller are given. The control input will be given in the body fixed frame, i.e., the control input for controlling pitch and roll in (4) will be given in body fixed coordinates. For the sake of this discussion we can assume that $\bar{a}$ in (4) can be controlled. However, a desired trajectory for controlling p_x and p_y is given in world coordinates. Therefore, to define tracking errors and control inputs, either the trajectory must be converted into body fixed coordinates or the control input must be converted into world coordinates. Let us consider the latter case. Then, if the ψ angle is known one can simply write

$$\begin{bmatrix} \bar{a}_x \\ \bar{a}_y \end{bmatrix} = R_z(\psi)^{-1} \begin{bmatrix} \tilde{a}_x \\ \tilde{a}_y \end{bmatrix}, \tag{6}$$

and (5a) (5b) will reduce to two (three dimensional) double integrators with control input:

$$u = \begin{bmatrix} \tilde{a}_x \\ \tilde{a}_y \end{bmatrix}. \tag{7}$$

However, if the ψ angle is not known the true model is

$$\begin{bmatrix} \dot{p_x} \\ \dot{p_y} \end{bmatrix} = \begin{bmatrix} v_x \\ v_y \end{bmatrix} \tag{8a}$$

$$\begin{bmatrix} \dot{v}_x \\ \dot{v}_y \end{bmatrix} = \underbrace{\begin{bmatrix} c_{\psi_e} & -s_{\psi_e} \\ s_{\psi_e} & c_{\psi_e} \end{bmatrix}}_{R_z(\psi)} \begin{bmatrix} \overline{a}_x \\ \overline{a}_y \end{bmatrix}, \tag{8b}$$

where $\psi_e = \psi - \hat{\psi}$ is the estimation error and $\hat{\psi}$ is the estimate. This will lead to position errors, i.e., angle estimation errors will lead to position errors. The estimations of the angles are done by the sensors in the Inertial Measurement Unit (IMU) of Quadcopters. In case of faulty sensor measurement, the estimation error will be non-zero which, thus, leads to errors in position. It is therefore very important to obtain accurate yaw estimates.

D. Sensor Modelling

The IMU consists of an accelerometer, gyroscope and a magnetometer [15].

The accelerometer measures the accelerations in $\{B\}$ and is defined as:

$$a_{IMU} = R^{\top}(\dot{v} - g\vec{e_3}) + b_a + \eta \in \{B\}, \tag{9}$$

where b_a and η denote a bias term and additive noise, respectively. The accelerometer is highly sensitive to vibration sources such as vibrations due to motors and propellers. Therefore, the raw accelerometer data should be low-pass filtered.

The gyroscope measures the angular velocities of the quadcopter in $\{B\}$ and is denoted as:

$$\Omega_{IMU} = \Omega + b_{\Omega} + \eta \in \{B\}, \tag{10}$$

where Ω_{IMU} are the angular velocities of the Quadcopter measured by the IMU, b_{Ω} and η denote a constant or time varying bias and additive noise respectively. The gyroscopes installed on a quadcopter are robust to noise and reliable. However, in order to estimate the angles of a quadcopter with the gyroscope, the output should be integrated over time. Due to this integration, the constant or time-varying bias is also integrated which causes the angle estimation to drift.

The magnetometer measures the ambient magnetic field with respect to $\{I\}$ and is denoted as:

$$m_{IMU} = R^{\top A}m + B_m + \eta_b \in \{B\}, \tag{11}$$

where ${}^{A}m$ is the Earth magnetic field in $\{I\}$, B_m is local magnetic disturbance and η_b is additive noise. The noise in the magnetometer is relatively low while the local magnetic disturbances can be high. In [1], [2], [3], [10] one can see the effect of magnetic field distortion on the angle estimation. The magnetic field is sensitive for hard iron and soft iron distortions, distortions due to charged wires and ferromagnetic materials. These distortions can lead to estimation errors up to 16 degrees which propagates to the overall quadcopter flight performance.

The attitude estimations for the roll, pitch and yaw angle from the accelerometer and the magnetometer measurements are given by:

$$\phi = \arctan2(a_y, a_x) \ \in \{B\}, \tag{12a}$$

$$\theta = \arctan2(a_x, \sqrt{a_y^2 + a_z^2}) \ \in \{B\}, \tag{12b}$$

$$\psi = \arctan2(B_y, B_x) \ \in \{B\}, \tag{12c}$$

where we express the magnetometer output from $\{I\}$ to $\{B\}$ as:

$$\begin{bmatrix} B_x \\ B_y \\ B_z \end{bmatrix} = (R_y(\theta)R_x(\phi))^{\top} \begin{bmatrix} M_x \\ M_y \\ M_z \end{bmatrix}. \tag{13}$$

The attitude estimations by integrating the gyroscope are denoted as:

$$\lambda_g(t) = \int_0^t \Omega_{IMU}(\tau)d\tau, \tag{14}$$

where $\lambda_g(t)$ are the estimations for roll, pitch and yaw. Substituting equation (10) in (14), we see that the integration includes the gyroscope bias which causes the angle estimation to drift. In Fig. 1, the different estimation methods using vector measurements, gyroscope measurements and distorted vector measurements can be seen. We can see that the vector measurements are relatively noisy, however, they do not drift like the gyroscope measurements. We can also see that the distorted vector measurements result in high errors during distortion.

The reliability of sensors in the IMU are essential for good angle estimations. Since all sensors have their advantages and disadvantages, Sensor Fusion Algorithms (SFAs) are used to combine the advantages of the sensors for angle estimations. In this research, we will focus on the widely used Complementary Filter as the main SFA [12].

E. Complementary Filter

A Complementary Filter (CF) fuses sensors with high frequency noise and low frequency disturbances [12], [13]. The CF can be represented with the block diagram in Fig 2, where λ_v is the vector measurement, λ_m is the magnetometer measurement and Ω is the gyroscope measurement. We can now define the dynamics of the filter as:

$$\dot{\hat{\lambda}} = \Omega + C(s)(\lambda_v - \hat{\lambda}), \tag{15}$$

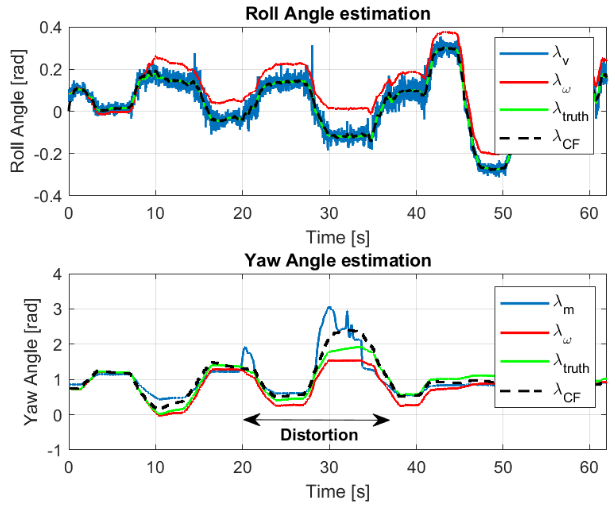

Fig. 1: Roll and Yaw estimation based on accelerometer and magnetometer as measurements and gyroscope measurements. Here,λ_v is the angle obtained by the vector measurements, λ_m is angle obtained by the magnetometer and λ_ω is the angle obtained by the gyroscope, λ_{CF} is the angle obtained by the complementary filter approach and λ_{truth} is the ground truth. The data is obtained by using a Pixhawk Module and reading IMU sensor data. The Ground Truth is obtained by the undisturbed Pixhawk Measurement

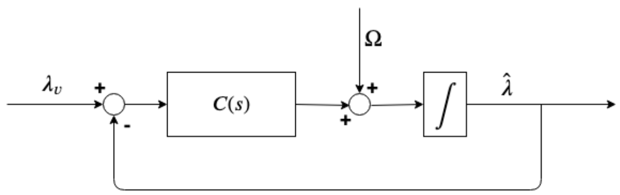

Fig. 2: Block Diagram of the Complementary Filter (CF)

where $C(s)$ is the control gain. Now rewriting in frequency domain, we can get the transfer functions of the filters,

$$\hat{\lambda}(s) = \underbrace{\frac{C(s)}{s + C(s)}}_{F_1(s)} \lambda_v(s) + \underbrace{\frac{s}{s + C(s)}}_{F_2(s)} \left(\frac{\Omega(s)}{s}\right), \qquad (16)$$

where $F_1(s)$ and $F_2(s)$ are the closed-loop complementary sensitivity and the sensitivity function respectively in which $F_1(s) + F_2(s) = 1$. The control gain $C(s)$ can be designed by classical control techniques. The simplest choice for the control gain is a proportional gain where $C(s) = k_p$. The complementary filters can now be written as:

$$F_1(s) = \frac{k_p}{s + k_p}, \qquad (17a)$$

$$F_2(s) = \frac{s}{s + k_p}, \qquad (17b)$$

where the crossover frequency is at $k_p[rad \cdot s^{-1}]$. With these filters, the complementary filter is weighing between the vector measurements and the gyroscope measurements. By choosing a crossover frequency, we can filter the high frequency noise of the vector measurement and combine this with an accurate low bandwidth rate measurements. The advantages of both measurements are combined to get the best estimation possible. In Fig 1, we can see the estimation for the Roll angle and the Yaw angle using the CF. As we can see, the angle estimation for the roll angle is accurate while the angle estimation for the yaw angle is not accurate during the distortion.

For the Complementary Filter of Mahony as designed in [12], we can conclude that a proportional gain is sufficient for compensating high frequency noise and gyroscope drift in the accelerometer and gyroscope fusion. For the magnetometer, the proportional gain strategy does not perform well when the magnetic field is being distorted. In this case, there is a constant weighing between the magnetometer and the gyroscope measurements. In [13], an adaptive gain has been proposed in order to cope with disturbances in the vector measurements. This has been tested for the pitch angle in which the results were promising. In our case, we focus on the estimation for the yaw angle in which the magnetometer is disturbed. In [11], we can find that the ideal attitude estimator should have three properties namely:

- An estimation for the angles
- Gyroscope bias correction
- Adaptivity for disturbances

In [17], one can see that a Kalman Filter has been proposed for attitude estimation. This resulted in a Root Mean Square Error (RMSE) of 0.2 degrees. The Kalman Filter is used as an optimal state observer. For the yaw estimation, we will use the Kalman filter as an independent estimator for yaw which will then be an input to our SFA.

F. Kalman Filter

The dynamics of a system in state-space can be defined as:

$$\dot{x}(t) = Ax(t) + Bu(t), \qquad (18a)$$

$$y = Cx(t) + Du(t), \qquad (18b)$$

where $x(t)$ and $u(t)$ are the state vector and the input vector respectively. The matrices A, B, C and D are the state matrix, input matrix, output matrix and the feedthrough matrix respectively. In case of the system dynamics are time-varying, one can write the Linear Time-Varying (LTV) system as:

$$\dot{x}(t) = \Phi(t, t_0)x(t) + Gw(t), \qquad (19a)$$

$$y = Cx(t) + v(t), \qquad (19b)$$

where $w(t)$ and $v(t)$ are the process noise and the measurement noise respectively. $\Phi(t)$ is the State-Transition-

Matrix (STM). The solution for the LTV-system when $w(t) = 0 \;\; \forall t$ can be denoted as:

$$x_i(t) = e^{\int_{t_0}^{t} A(\tau)d\tau} x_i(0), \tag{20}$$

where $x_i(0)$ are the initial values of the state vector. From equation (20), the STM is then defined as:

$$\Phi(t, t_0) = e^{\int_{t_0}^{t} A(\tau)d\tau}. \tag{21}$$

The noise is assumed to be uncorrelated in time and thus is a white noise and has zero mean [17]. The covariances of the noise can be denoted as:

$$\mathbb{E}\left\{ \begin{bmatrix} w(t) \\ v(t) \end{bmatrix} \begin{bmatrix} w(\tau)^{\intercal} v(\tau)^{\intercal} \end{bmatrix} \right\} = \begin{bmatrix} Q & S \\ S^{\intercal} & R \end{bmatrix} \delta(t-\tau), \tag{22}$$

where Q and R are the tuning knobs in which a small Q indicates that we are confident about the model and a small R indicates that we are confident about the measured output i.e. the sensors. S is the cross correlation matrix which is assumed to be zero and $\delta(t-\tau)$ is the Kronecker Delta where $\delta(0) = 1$ if $t = \tau$ and 0 otherwise. Furthermore, the initial state is assumed to be Gaussian and characterized by:

$$\mathbb{E}\{x_i(0)\} = x_i(0), \tag{23a}$$
$$\mathbb{E}\{(x_i(0) - \hat{x}_i(0))(x_i(0) - \hat{x}_i(0))^{\intercal}\} = P_0, \tag{23b}$$

where $\hat{x}(0)$ is the initial value of the estimation and P_0 is the initial value of the state covariance matrix. The objective of the Kalman Filter is to find an estimate such that we minimize a linear function of the steady state error covariance. One can define the estimation by a Kalman Filter as:

$$\dot{\hat{x}}(t) = \Phi(t)\hat{x}(t) + K(t)(y - C\hat{x}(t)), \tag{24}$$

where $\hat{x}$ is the state-estimation, $(y - C\hat{x}(t))$ is the estimation error and $K(t)$ is the Kalman Filter gain which minimizes the error which is denoted by [18]:

$$K(t) = P(t)C^{\intercal}R^{-1}, \tag{25}$$

in which $P(t)$ is the state covariance matrix and can be obtained by solving the Algebraic Riccatti Equation (ARE) for LTV systems [17], [18]:

$$\dot{P}(t) = \\ AP(t) + P(t)A^{\intercal} + GQG^{\intercal} - P(t)C^{\intercal}R^{-1}CP(t). \tag{26}$$

The Kalman Filter gain minimizes a linear function of the state covariance error such that the estimation error is converging to the real state. The estimation error of the Kalman Filter is defined as:

$$e(t) = x(t) - \hat{x}(t), \tag{27}$$

where $\hat{x}(t)$ is the state estimation. The error propagation can be defined by:

$$\begin{aligned} \dot{e}(t) &= \dot{x}(t) - \dot{\hat{x}}(t), \\ &= (A - KC)(x(t) - \hat{x}(t)). \end{aligned} \tag{28}$$

In order to obtain a converging error, the pair (A, C) must be observable. In case the system is unobservable, we can not retrieve the state estimations with a Kalman Filter. The notion for observability, however, in case of LTV-systems is not the same as in case of a time-invariant system. In [17], one can see a Kalman Filter approach on state estimation for an Inertial Navigation System (INS) for indoor position and attitude estimation. In case of a completely observable system, the Kalman Filter estimates the heading with an RMSE of 0.2 degrees. However, the output matrix which consists of the position measurements only appear to be unobservable and state estimations can not be found. In our case, only the position measurement is available. Therefore, the proposed model should be observable for all inputs with the position measurements as outputs in order to obtain reliable estimations.

G. Motivation

In [1], [2], [3], one can see that magnetic disturbances lead to high errors in ψ-estimation. In Section II-C, one can find the role of ψ-estimation and how it can lead to errors in position. Due to disturbances in magnetic field, this leads to errors in ψ-estimation which in its turn lead to errors in position which influences the overall performance of flight. In Section II-D, the sensors and how the sensors are used are described for attitude estimation. This has directly been coupled to Section II-E in which the Complementary Filter has been described. The conventional method of Mahony fails to handle magnetic failures as can be seen in Fig 1. Due to this reason, an adaptive method has been proposed in [13] to handle errors in accelerometer for pitch estimation. However, for ψ-estimation, this has not been tested. In [17], one can find a Kalman Filter estimation for ψ-estimation which gives promising results. However, in order to get these results, the system must provide the position, velocity and the heading as a measurement which is not true in the case of a Quadcopter. In [11], we can see that the ideal SFA contains an estimation, gyroscope bias correction and adaptivity.

This motivates us to extend the adaptive filter proposed in [13] with a Kalman Filter estimation. The adaptive filter adapts such that the system switches between the Kalman Filter and magnetometer based on the magnetic field distortion and based on the observability property. This is then again being adapted based on the similarity property between a vector measurements and the gyroscope angle estimation as proposed in [13] to get a more robust system for ψ-estimation in case of magnetic field distortion or unreliable magnetometer sensor.

III. KALMAN FILTER BASED ψ-ESTIMATION

The model for the Kalman Filter estimation can be described as:

$$\dot{x}(t) = A(t)x(t), \tag{29a}$$
$$y = Cx(t), \tag{29b}$$

where $x(t) \in R^n$ is the state vector, $A(t) \in \mathbb{R}^{n\times n}$ is the time-varying state matrix and C is the output matrix. The state vector $x(t)$ is defined as $[p_x, p_y, v_x, v_y, c, s]^\intercal$ where:

$$c = \cos(\psi), \tag{30a}$$
$$s = \sin(\psi), \tag{30b}$$

in which the time derivative of these states are defined as:

$$\dot{c} = -\dot{\psi}\sin(\psi), \tag{31a}$$
$$\dot{s} = \dot{\psi}\cos(\psi), \tag{31b}$$

where we can approximate Equation (1c) for yaw as:

$$\dot{\psi} = \Omega_z, \tag{32}$$

where Ω_z is the third component of the angular velocity. Combining Equation (5a)(5b) and (31a)(31b) and writing in terms of equation (29a)(29b), we can obtain the Kalman Filter model as:

$$\begin{bmatrix} \dot{p}_x \\ \dot{p}_y \\ \dot{v}_x \\ \dot{v}_y \\ \dot{c} \\ \dot{s} \end{bmatrix} = \underbrace{\begin{bmatrix} 0 & 0 & 1 & 0 & 0 & 0 \\ 0 & 0 & 0 & 1 & 0 & 0 \\ 0 & 0 & 0 & 0 & \bar{a}_x(t) & -\bar{a}_y(t) \\ 0 & 0 & 0 & 0 & \bar{a}_y(t) & \bar{a}_x(t) \\ 0 & 0 & 0 & 0 & 0 & -\Omega_z(t) \\ 0 & 0 & 0 & 0 & \Omega_z(t) & 0 \end{bmatrix}}_{\text{A(t)}} \begin{bmatrix} p_x \\ p_y \\ v_x \\ v_y \\ c \\ s \end{bmatrix}, \tag{33a}$$

$$y = \underbrace{\begin{bmatrix} 1 & 0 & 0 & 0 & 0 & 0 \\ 0 & 1 & 0 & 0 & 0 & 0 \end{bmatrix}}_{\text{C}} x, \tag{33b}$$

in which we define the position as the only sensor outputs in the measurement model. From Equation (33), we can find estimations for c and s. From these estimations, we can find an estimation for ψ as:

$$\hat{\psi} = \begin{cases} \tan^{-1}\left(\frac{\hat{s}}{\hat{c}}\right); & \hat{s} \geq 0,\ \hat{c} > 0, \\ \frac{\pi}{2}; & \hat{s} > 0,\ \hat{c} = 0, \\ \pi + \tan^{-1}\left(\frac{\hat{s}}{\hat{c}}\right); & \hat{c} < 0. \end{cases} \tag{34}$$

Contrarily to [17], instead of having $\cos(\psi)$ and $\sin(\psi)$ in the state matrix $A(t)$, we use them as states in order to make an estimation of c and s to estimate the ψ-angle. This decreases the overall complexity since we do not have to handle non-linear terms in the state matrix. The result of the ψ-estimation for the Quadcopter can be seen in Figure 3.

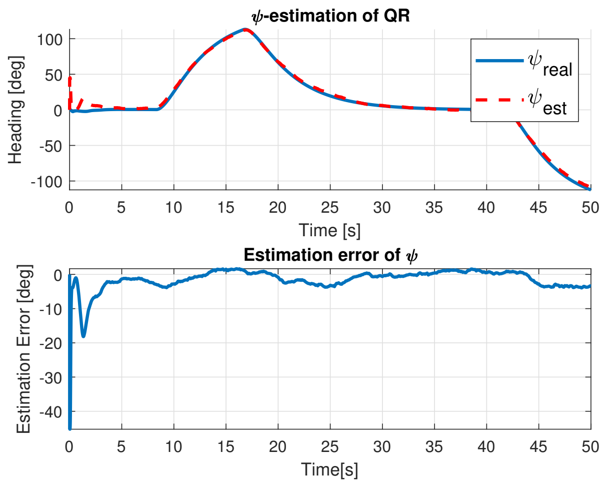

Fig. 3: ψ-estimation based on Kalman Filter estimation. Circular motion trajectory in which the ψ-angle has been bounded between $[-\pi, \pi]$

We see that the Kalman Filter estimation converges to the real angle. The RMSE for this estimation is equal to 3.5 degrees. We can observe that the estimation has a large error during initialization. As discussed in Section II-F, a system which is weakly observable or unobservable does not have a converging error. In Section III-A, we will discuss the observability of the proposed system.

A. Observability Analysis

The notion for observability for Linear Time-Invariant (LTI) systems is given by the standard observability matrix in control theory denoted as $O_{LTI} = \begin{bmatrix} C^\intercal & (CA)^\intercal & (CA^2)^\intercal & \ldots & (CA^{n-1})^\intercal \end{bmatrix}^\intercal$. The system in LTI is observable if the observability matrix has rank n or is full rank. This does not hold in case of LTV systems since the state matrix $A(t)$ changes over time. For LTV-systems, the notion of observability can often be inferred from the observability gramian [14], [19], [20]:

$$W_o = \int_{t_0}^{t} (\Phi(t,t_0)^\intercal C^\intercal C \Phi(t,t_0))dt, \tag{35}$$

where $\Phi(t)$ is the State Transition Matrix (STM) which can be determined as defined in Equation (21). The system is observable if and only if the observability gramian is full rank for all times t. We can also determine local observability by analyzing the system between arbitrary bounds between $[t, t_0]$. In order to analyze the effects of the inputs $[\bar{a}_x, \bar{a}_y, \Omega_z]^\intercal$ on the observability, two tests in simulation have been conducted. In one test, the Quadcopter is brought to a certain setpoint and remains hovering while in the other test, the Quadcopter flies a circular motion in which the accelerations are not constant. The initial values are

$[\bar{a}_x, \bar{a}_y, \Omega_z]^\intercal = [0, 0, 0]$. The results are given in Fig 4a and 4b. We can see that the observability gramian is full rank in case the inputs are nonzero. The critical inputs hereby are the accelerations $\bar{a}_x$ and $\bar{a}_y$. The angular velocity Ω_z changes constantly over time, but does not contribute to the overall observability. We can see that during initialization, the system is not observable. We can, thus, directly link this to the high estimation error as seen in Fig 3. After the initialization, we can see that the Kalman Filter estimation is converging. From this, we can conclude:

$$\rho(W_0) = \begin{cases} 6, & \text{if } [\bar{a}_x, \bar{a}_y] \neq [0, 0] \quad \forall t \\ 4, & \text{otherwise} \end{cases}, \tag{36}$$

where $\rho(W_0)$ denotes the rank operator. The effect of the inputs on the observability are now analyzed. We can now tell when the system is observable i.e. the Kalman Filter is converging. However, the accuracy of the estimation and the sensitivity to measurement noise depends on the singularity of the observability gramian i.e. the Degree of Observability (DoO)

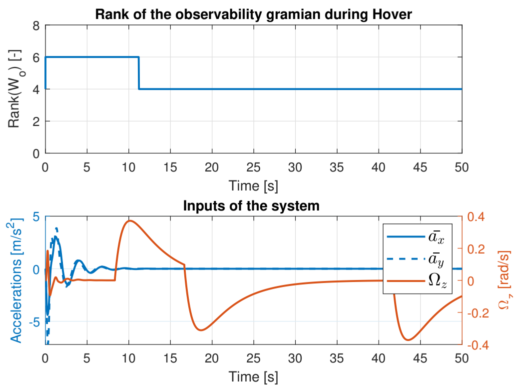

(a) Observability during hovering

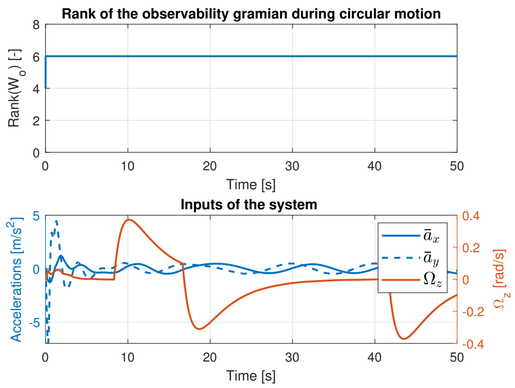

(b) Observability during circular motion

Fig. 4: Observability test in simulation with model inputs $[\bar{a}_x, \bar{a}_y, \Omega_z]^\intercal$ during hover and circular motion

B. Degree of Observability

In Section III-A, we have analyzed the effect of the inputs on the observability of the system. The accuracy of the estimation depends highly on the singularity of the observability gramian [21]. In [21], we can see the increasing accuracy of the estimation by a decreasing error covariance due to an increase in DoO, to be defined shortly. The DoO will be used as an adaptation parameter for the adaptive complementary filtering method. In [22], [23], [21], several methods have been discussed in order to determine the DoO. For this research, we base our work on the Singular Value Decomposition (SVD) method where we determine the condition number of the observability gramian. The condition number shows how close a matrix is to being singular. A large condition number states that a matrix is nearly singular while a low condition number states that a matrix is far from singular. We can use this property to define the DoO as:

$$\delta_o(t) = \frac{1}{\kappa(W_o)} = \frac{|\sigma_{min}(W_0)|}{|\sigma_{max}(W_0)|}, \tag{37}$$

where σ is the maximum and minimum singular value of W_o and $\kappa(W_0)$ is the condition number of the observability gramian. Due to the fact that we invert the condition number, we can define a bound for the DoO which is $0 \leq \delta_o(t) \leq 1$. If the DoO is close to zero, the condition number is high which states that the matrix is nearly singular and the DoO is thus low. In the opposite case, the DoO is high when the condition number is low and $\delta_o(t)$ is close to one. The DoO with respect to the inputs $[\bar{a}_x, \bar{a}_y, \Omega_z]^\intercal$ can be found in Figure 5. We can see in Figure 5 that the DoO in Figure 5a is close to zero in case of inputs $\bar{a}_x$ and $\bar{a}_y$ are close to zero as expected. In case of a motion, the acceleration terms become nonzero and this results in a higher DoO. The contribution of the gyroscope is also visible now in Figure 5b. The effect of the DoO on the estimation error as defined in Equation (27), is given in Figure 6.

Here we can clearly see the effect of the non converging estimation due to a low DoO. The error in hovering motion with low DoO due to low accelerations is drifting from the real estimation while the error in circular motion with relatively higher DoO remains bounded. We can, thus, conclude that the DoO is of great importance for the estimation accuracy.

In adaptive filtering, the main objective is to weigh the vector measurements and estimation based on properties such as magnetic field distortion and Degree of Observability. We can now form a filter which weighs between the vector measurement and the Kalman Filter estimation is based on the DoO. This adaptive filter will be elaborated in the next section.

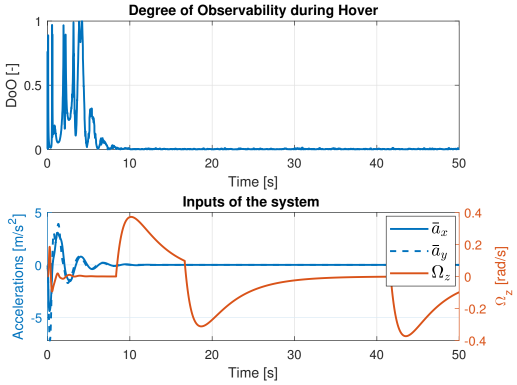

(a) DoO during hovering

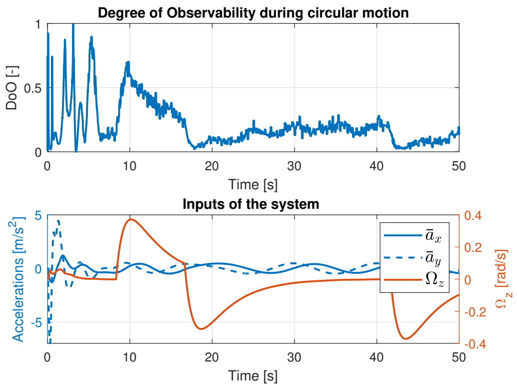

(b) DoO during circular motion

Fig. 5: DoO test in simulation with model inputs $[\bar{a}_x, \bar{a}_y, \Omega_z]^\intercal$ during hover and circular motion

IV. ADAPTIVE FILTERING

A. Adaptive Complementary Filter

The complementary filter as proposed by Mahony has been described in Section II-E. This filter has a static gain which weighs the gyroscope integration with respect to the vector measurement. In case of ψ-estimation, the vector measurements are the magnetometer measurements. The adaptive filter has been introduced in [13] in which an adaptation logic has been designed based on similarity property of the estimations. In [13], however, only the pitch angle has been considered in which distortions in accelerometer measurements have been handled. The block diagram for the complementary filter has been given in Fig 2. For ψ-estimation, we propose a complementary filter which is adaptive to handle distortions in magnetometer measurements, which handles gyroscope bias and which has an estimation. The overall block diagram is given in Fig 7. In Fig 7, λ_m and λ_k are the angle estimation by magnetometer measurements and ψ-estimation by Kalman Filter respectively, $\hat{\lambda}$ is the angle estimation by the filter, Ω_z is the angular velocity by gyroscope measurement, $\alpha(t)$, $\beta(t)$ and $\gamma(t)$ are the adaptive gains. We can now write the dynamics of the filters as described in Equation 15:

$$\dot{\hat{\lambda}} = \Omega_z + \alpha(t)(\lambda_{mk} - \hat{\lambda}), \tag{38}$$

where λ_{mk} is the angle estimation by the combination of the magnetometer measurement and the Kalman Filter estimation. We can write this as:

$$\dot{\hat{\lambda}} = \Omega_z + \alpha(t)(\underbrace{(\beta(t)\gamma(t)\lambda_m + (1-\beta(t)\gamma(t))\lambda_k)}_{\lambda_{mk}} - \hat{\lambda}). \tag{39}$$

The Kalman Filter estimation λ_k is being weighed with respect to the magnetometer measurement by $\beta(t)$ in case of no magnetic distortions. This results in a new measurement λ_{mk} which in its turn is weighed with respect to the gyroscope integration by $\alpha(t)$. In case of magnetic distortions, the magnetometer is completely shut off by $\gamma(t)$ which results in $\lambda_{mk} = \lambda_k$. This is then again weighed by $\alpha(t)$. We have three types of adaptation rules namely:

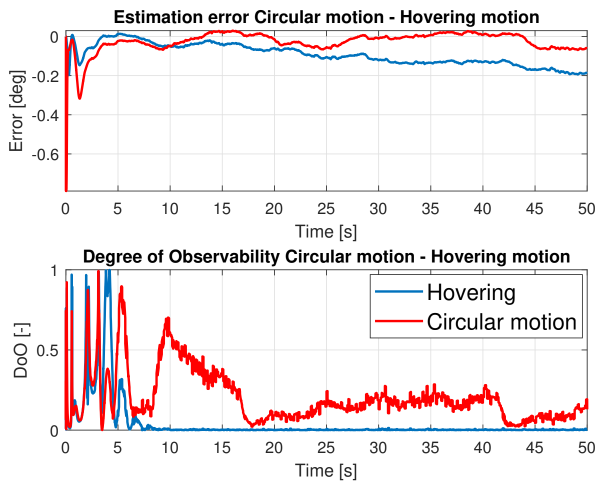

Fig. 6: Estimation error in circular motion with high DoO and estimation error in hovering motion with low DoO

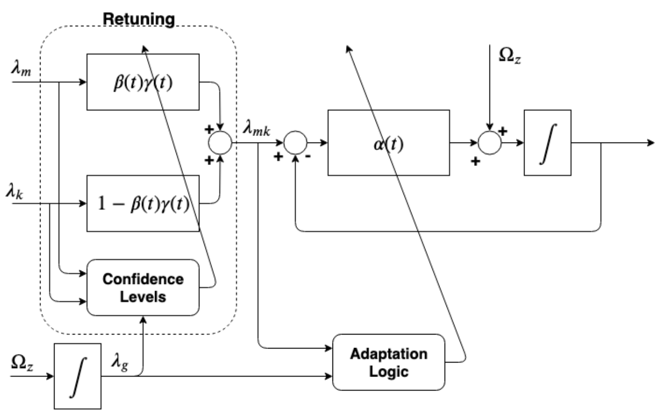

Fig. 7: Overall block diagram of the proposed adaptive complementary filter

- $\alpha(t)$ adaptation based on similarity as discussed in [13]
- $\beta(t)$ adaptation based on Degree of Observability (DoO) to qualify the KF-GPS
- $\gamma(t)$ adaptation based on the magnetic field distortion to switch between raw magnetometer estimation and KF-GPS

The adaptation based on similarity is defined a similarity between the angle estimation based on gyroscope integration and the angle estimation based on the magnetometer measurement over a moving time window. If the angles obtained by the measurements are similar, the sensors are realiable. The similarity measure can be defined as [13]:

$$S(t) = \min(\bar{S}, \min_c J(c,t)), \tag{40}$$

where $0 \leq \bar{S} \leq \infty$ is the upper bound of the similarity measure and $J(c,t)$ is the cost function which compares the two signals by shifting them on top of each other over a moving time window:

$$J(c,t) = \sqrt{\int_{t-h}^{t} (\lambda_{mk}(\tau) - \lambda_g(\tau) - c)^2 d\tau}, \tag{41}$$

where λ_g is the angle estimation by gyroscope integration, h is the window length in the interval $\tau \in [t-h, t]$ and c is the estimation of the bias by gyroscope integration. The latter corrects the gyroscope bias such that both signals are shifted on top of each other. This is done by taking the mean value of the two measurements over a window length:

$$c(t) := \arg\min_c J(c,t) = \frac{1}{h}\int_{t-h}^{t} (\lambda_{mk}(\tau) - \lambda_g(\tau)) d\tau. \tag{42}$$

We can see the effect of this in Fig. 8. We can now define

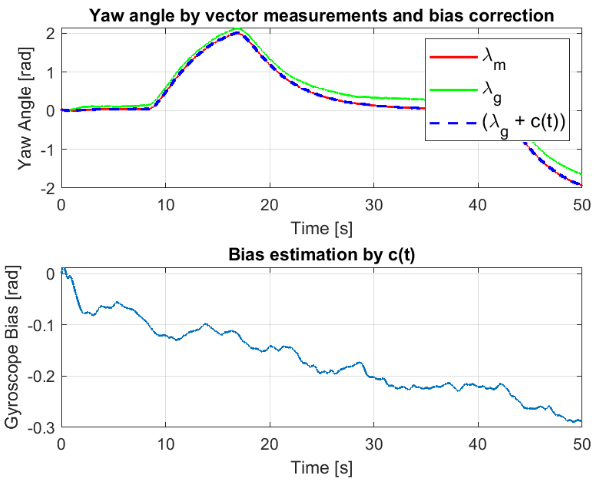

Fig. 8: Shifting the magnetometer angle estimation and the gyroscope integration on top of each other by $c(t)$ bias correction (no distortion)

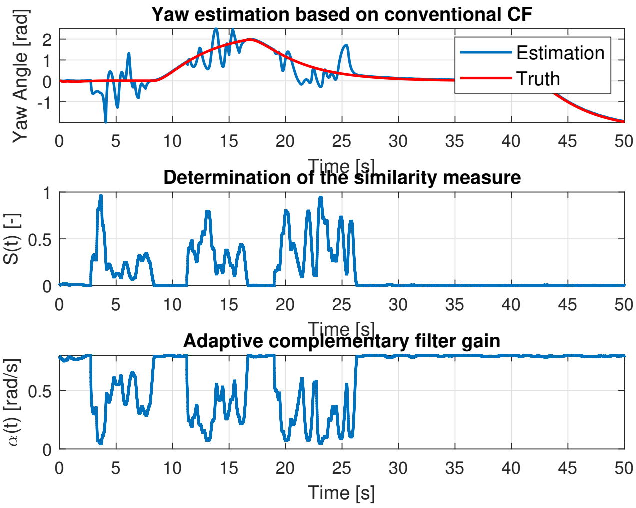

Fig. 9: **Top** Disturbed conventional complementary filter estimation **Middle** Determination of $S(t)$. **Bottom** The adaptive $a(t)$ gain which reacts to disturbances.

the adaptive control gain as:

$$\alpha(t) = \bar{a}\exp^{-K_\alpha S(t)}, \tag{43}$$

where $\bar{a} > 0$ and $K_\alpha > 0$ in which $\bar{a}$ is the gain which determines the initial starting value of the adaptive gain. By varying K_α, we can ensure quick reaction to disturbances. This reaction to disturbances can be seen in Fig 9. In case of no distortion $\alpha(t)$ is close to one which indicates that the magnetometer measurement is weighed with respect to the gyroscope integration evenly. However, in case of distortion, the adaptive filter is close to zero which indicates that more emphasis has been put on the gyroscope integration in case of distortion. We can also see that the adaptive filter does not shut off the magnetometer measurement. It does take into account some degree of distortion in the measurement. Therefore, in order to cope with this, the Kalman Filter estimation is essential.

Assume the magnetometer sensor is not distorted by external factors. In this case, we have λ_{mk} as defined in Equation (39) and thus $\gamma(t) = 1$. Since we trust the magnetometer measurement and we have the Kalman Filter estimation for redundancy, we have to qualify the Kalman Filter based on the DoO as described in section III-B. The upperbound of $\delta_o(t)$ is equal to 1. The adaptation logic for $\beta(t)$ is based on the value of $\delta_o(t)$. Hereby the deflection from the maximum value of $\delta_o(t)$ is of importance. The same strategy as in Equation (41). We can, thus, define the cost function as:

$$D(t) = \sqrt{\int_{t-h}^{t} (1 - \delta_0(\tau))^2 d\tau}, \tag{44}$$

where $\delta_o(\tau)$ is the Degree of Observability (DoO).

Here, we compare the DoO with respect to its maximum value. The adaptive gain now becomes:

$$\beta(t) = 1 - \bar{\beta}\exp^{K_\beta D(t)}, \tag{45}$$

where $\bar{\beta} > 0$ is the initial value of the gain and $K_\beta > 0$ is the control gain to tune sensitivity towards changes in $D(t)$. Assuming that the DoO is close to zero, i.e. weakly observable, Equation (44) becomes equal to approximately 1. In this case, Equation (45) shows that 0.63 or 63 % of the original signal is kept. Therefore, we can tune this percentage with K_β. An exponential function is used as exponential smoothing. In case of very noisy sensors or outliers, the exponential smoothing function as a confidence level can cope with these types of disturbances. In case of a high DoO i.e. strong observable, Equation (44) becomes close to zero. This results in Equation (45) to becomes close to zero which results in more confidence on the KF-GPS method. The result for a circular motion is given in Fig 10.

We can see how the filter reacts upon the DoO being lowered. The adaptive gain $\beta(t)$ becomes close to one which results in putting more emphasis on λ_m instead of λ_k. In the contrary case, we see that during high DoO, we see that the magnetometer measurement is taken less into account with respect to the Kalman Filter estimation. The Kalman Filter estimation of ψ aids the magnetometer measurement. In this case, however, we assume that the magnetometer is not distorted. In case of a distorted magnetometer, we want to shut off the magnetometer and rely on the Kalman Filter estimation without taking into account the DoO. We then want to weigh λ_k with respect to Ω_z.
To determine whether the magnetometer measurement is distorted or not, we have defined the gain $\gamma(t)$. In

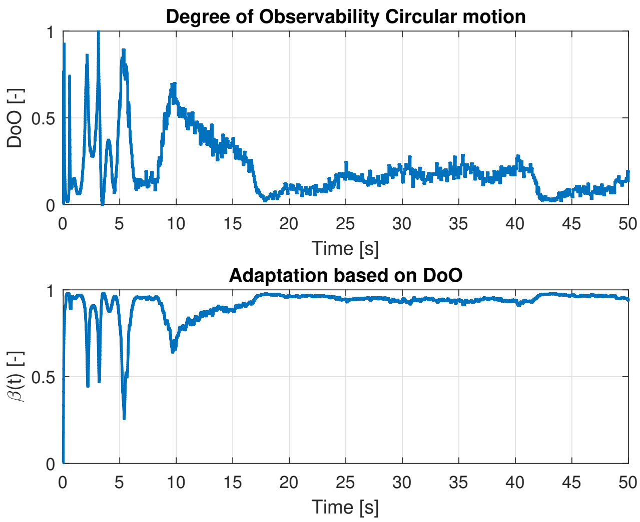

Fig. 10: The adaptive $\beta(t)$ gain which weighs between the magnetometer and the Kalman Filter estimation

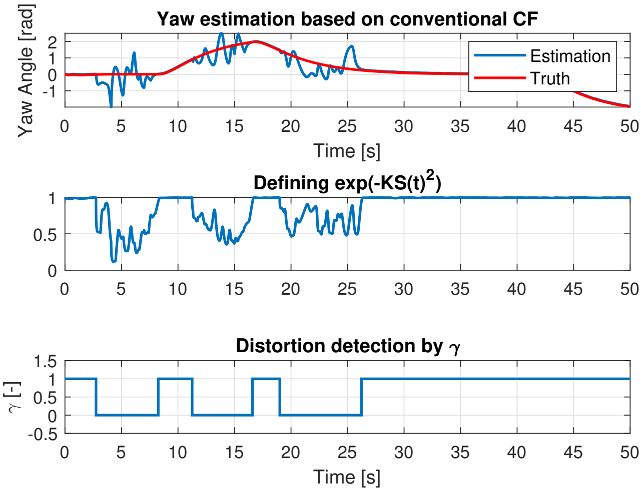

Fig. 11: **Top** Estimating ψ by conventional Complementary Filter. **Middle** Estimation of $\exp^{-KS(t)^2}$ **Bottom** Determination of $\gamma(t)$ and its reaction on distortions

case the magnetometer is distorted, the measurement is immediately shut down i.e $\gamma(t) = 0$. If this is the case, $\lambda_{mk} = \lambda_k$ in which we rely on the Kalman Filter. In case the estimation is not reliable, we use the adaptive gain $\alpha(t)$ to adapt with respect to the gyroscope integration. In [1], we see how we can determine magnetic disturbance in case of dynamic movement. We have also used this strategy to tune our filter. In [1], the following equation is used to determine the distortion:

$$\bar{\lambda}_d = \frac{1}{h}\int_{t-h}^{t} (\lambda_m(\tau) - \lambda_g(\tau))d\tau, \tag{46}$$

where $\bar{\lambda}_d$ is the difference difference between the magnetometer and gyroscope measurement which is averaged over a sliding window with window length h. We can thus define the distortion detection as:

$$\gamma(t) = \exp^{-K\bar{\lambda}_d^2}. \tag{47}$$

The method in [1] works with a threshold method. In case of no distortion, Equation (46) is close to zero. To handle disturbances and sensor noise, we use an exponential function such that in case of no distortion, the confidence level $\gamma(t)$ becomes equal to 1. Therefore, the calibration measure σ_{max} is equal to 1 in case of no distortion. In case of distortion, the signal will differ from this maximum value. We can define the distortion detection as:

$$\gamma(t) = \begin{cases} 0, & \text{if } e^{-K\bar{\lambda}_d^2} < \sigma_{max} \\ 1, & \text{otherwise,} \end{cases} \tag{48}$$

where σ_{max} is the calibrated measure in case of no distortion. We can now directly see the distortion detection in Fig 11. In Fig 11, we can see that the method as proposed can detect the distortions well without misfires. We see that $\gamma(t)$ becomes zero in case of distortion and one otherwise as described in Equation 48. The effect of $\alpha(t), \beta(t)$ and $\gamma(t)$ can be found in section V.

B. Extending Adaptive Filter for R in SO(3)

In the previous method, we have assumed that the Roll angle ϕ and the Pitch angle θ are small. In order to get a good understanding of the attitude of the Quadcopter, we have to extend this one dimensional problem to a three dimensional problem. In order to do this, the attitude of the Quadcopter has to be determined by the rotation matrix R in the Special Orthogonal Group $SO(3)$. In the work of Mahony in [12], we can find three complementary filter based estimation methods for the rotation matrix. Here, we see three methods namely:

- Direct Complementary Filter (DCF)
- Passive Complementary Filter (PCF)
- Explicit Complementary Filter (ECF)

The *Direct Complementary Filter (DCF)* without bias correction can be written as [12]:

$$\dot{\hat{R}} = \hat{R}\Big(R_y(\Omega^y) + K_p\hat{R}\omega\Big)_\times, \quad \hat{R}(0) = \hat{R}_0 \tag{49a}$$

$$\omega = \mathbb{P}(\tilde{R}), \quad \mathbb{P} = \frac{1}{2}(\tilde{R} - \tilde{R}^\intercal), \tag{49b}$$

where ω is the correction term, $\tilde{R} = \hat{R}^\intercal R_y$, R_y is defined by the Tait-Bryant rotation convention described in Equation (2),$(.)_\times$ is the skew-symmertric matrix notation, K_p is the observer gain, Ω^y are the angular velocities in $\{B\}$ and $\hat{R}$ is the $R \in SO(3)$ estimation with $\hat{R}_0$ as the initial values. The disadvantage of this method is the fact that R_y has to be used in order to map the velocities of Ω^y into the inertial frame. In case R_y is faulty, the error term which is defined by:

$$E_{DFC} = \frac{1}{2}tr(\mathbb{I}_{3\times3} - \hat{R}^\intercal R_y), \tag{50}$$

where $\mathbb{I}_{3\times3}$ is the identity matrix, will not converge to zero. The errors in angle estimations as defined in Equation (12) will directly effect the estimation due to the coupled nonlinear dynamics.

Due to this disadvantage, the *Passive Complementary Filter (PCF)* has been developed. The dynamics are given as:

$$\dot{\hat{R}} = \hat{R}(\Omega^y_\times + K_p\omega), \tag{51a}$$

$$\omega = \mathbb{P}(\tilde{R}), \quad \mathbb{P} = \frac{1}{2}(\tilde{R} - \tilde{R}^\intercal). \tag{51b}$$

We can clearly see that R_y is now not used to map the velocities into $\{I\}$. However, this method introduced a new feedback loop. The stability has been proved in [12]. Another disadvantage is the still coupled dynamics in the PCF. In case K_p becomes adaptive, we can only make the system more robust by relying on the gyroscope integration which has a bias. Therefore, the PCF has been rewritten in [12] into the ECF such that the vector measurements are decoupled.

The *Explicit Complementary Filter (ECF)* decouples the vector measurement such that a faulty sensor can be switched off. The dynamics of the ECF are defined as:

$$\dot{\hat{R}} = \hat{R}\Big((\Omega^y)_\times + K_p(\omega_{mes})_\times\Big), \qquad \hat{R}(0) = \hat{R}_0 \tag{52a}$$

$$\omega_{mes} = \sum_{i=1}^{n} k_i v_i \times \hat{v}_i, \qquad k_i > 0 \tag{52b}$$

where k_i are the gains to put confidence levels on the vector measurements, v_i and $\hat{v}_i$ are the vector measurements and the estimated vector measurements respectively. We can directly see that we do not need R_y to construct the complementary filter. Only the direction of the vector measurements are of importance. Therefore, to ensure $|v_i| = 1$, let

$$v_i = R^\intercal \frac{v_{0i}}{|v_{0i}|} \quad v_i \in \{B\}, \tag{53a}$$

$$\hat{v}_i = \hat{R}^\intercal \frac{v_{0i}}{|\hat{v}_{0i}|} \quad \hat{v}_i \in \{B\}, \tag{53b}$$

where $v_{0i} \in \{B\}, i = 1, \ldots, n$, denote a set of n known inertial directions and $R^\intercal$ and $\hat{R}^\intercal$ are the rotation matrices in which $\hat{R}^\intercal$ is the estimation of the rotation matrix which depends on the gyroscope measurement. We can directly see the challenge with this filter. In case we want to add an extra measurement, name the KF-GPS, we have to transform KF-GPS from $\{I\}$ to $\{B\}$. This filter has only measurements in $\{B\}$. Due to time restrictions, we could not find a method to sum measurements from different frames. Therefore, we only base our first extension of the filter on making the control gains k_i adaptive such that we can handle distortions in magnetometer measurements and we discard the yaw estimate based on the position measurements.

We can now define the error of the measurement and the estimation as:

$$E_i = 1 - v_i^\intercal \hat{v}_i = \begin{cases} 1 - v_a^\intercal \hat{v}_a \in \{B\} \\ 1 - v_m^\intercal \hat{v}_m \in \{B\} \end{cases}, \tag{54}$$

where v_a and v_m are the accelerometer and magnetometer measurements. Recall Equation (44) where we used the DoO to make the control gain adaptive. The same metric can be applied in this case. Here, we use the error terms of the vector measurements as our adaptivity metric as:

$$E_a(t) = \sqrt{\int_{t-h}^{t} (1 - v_a^\intercal(\tau)\hat{v}_a(\tau))^2 d\tau}, \tag{55a}$$

$$E_m(t) = \sqrt{\int_{t-h}^{t} (1 - v_m^\intercal(\tau)\hat{v}_m(\tau))^2 d\tau}. \tag{55b}$$

Here, we analyze the mean value of both measurement errors over a moving time window h. We can now define the adaptive control gains as:

$$k_a = \bar{k}\exp^{-K_a E_a(t)}, \quad (56a)$$
$$k_m = \bar{k}\exp^{-K_m E_m(t)}, \quad (56b)$$

with $\bar{k} > 0$, $K_a > 0$ and $K_m > 0$ being the tuning parameters of the adaptive filters. From here, we can see that in case of no distortion, the errors terms for both measurements goes to zero. In this case, k_a and k_m are both equal to one and both measurements are used for the attitude estimation. In case of a distortion, the errors terms will differ from zero. By using an exponential function, we can filter noise from the measurements and we can tune the confidence levels with the control gains K_a and K_m In case both errors terms are equal to 0.5 and $\bar{k} = K_a = K_m$ are equal to one, the result will be a confidence of 60 percent of the orignial signal. By tuning the control gains K_a and K_m, we can lower this confidence level. This method gives the user more freedom to tune the adaptive filters.
Now we have proposed a metric to determine errors in measurements, we can now define a metric to qualify the performance of the adaptive filter. The error terms to qualify the quality of the measurements as defined in [12] is given as:

$$E_{mes} = k_a E_a + k_m E_m, \quad (57)$$

In case of the conventional method with a static gain for k_a and k_m, the measurement error would increase with increasing errors in the measurements. With k_a and k_m adaptive, we expect the total measurement error to converge to zero.

V. SIMULATIONS

In order to demonstrate the effectiveness of the proposed approach, simulations were performed to compare the conventional Complementary Filter (CF)[12], the Adaptive Filter (AF) as proposed in [13], KF-GPS as proposed in section II-F and the GPS aided Adaptive Complementary Filter (KF-ACF) as proposed in section IV-A. For all filters, we fly the same circular trajectory. The Quadcopter model starts from initial value and rises up to a certain height. From here, the Quadcopter fly in a circular motion and the ψ-angle is being varied from $[-\pi, \pi]$. The result of ψ-estimation by different filters can be found in Figure 12. We can clearly see the effectiveness of the KF-ACF. The KF-ACF outperforms the conventional CF, the adaptive AF and the KF-GPS. The KF-GPS, however, shows good performance. However, the filter will fail in case of a hovering motion. The Degree of Observability (DoO) will decrease which results in a drift in the estimation. The CF suffers from high errors due to distortions in magnetic field as expected. The AF shows good disturbance attenuation, however, due to the fact that we rely on the gyroscope integration during the magnetic field distortion, we see a small drift in angle estimation. We see that this drift is then compensated for in case of no distortion. In the case of KF-ACF, the estimation is robust against gyroscope integration drift and magnetic field distortion. In case the magnetometer fails, we rely on the gyroscope integration and the Kalman Filter estimation in which the Kalman Filter estimation KF-GPS already shows good results. The estimation error can be found in Figure 13. To quantify the results, the RMSE error has been calculated per method. The results can be found in Table I:

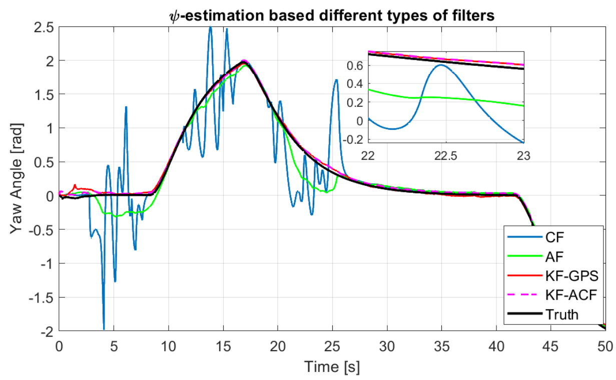

Fig. 12: Results of the effectiveness of the conventional Complementary Filter (CF), the Adaptive Filter (AF), Kalman Filter (KF-GPS) and the Kalman Filter aided Adaptive Complementary Filter (KF-ACF). For the KF-ACF, $\bar{\alpha} = 1[rad \cdot s^{-1}]$, $K_\alpha = 5[-], \bar{\beta} = 1[rad \cdot s^{-1}]$, $K_\beta = 4[-]$

Filter	RMSE [rad]	RMSE [deg]
CF	0.35	19.8
AF	0.14	7.9
KF-GPS	0.04	2.3
KF-ACF	0.03	1.7

TABLE I: RMSE values of the CF, AF, KF-GPS and the KF-ACF in radians and degrees

In Table I, we can see that the proposed method and the KF-GPS outperforms the other conventional filters.

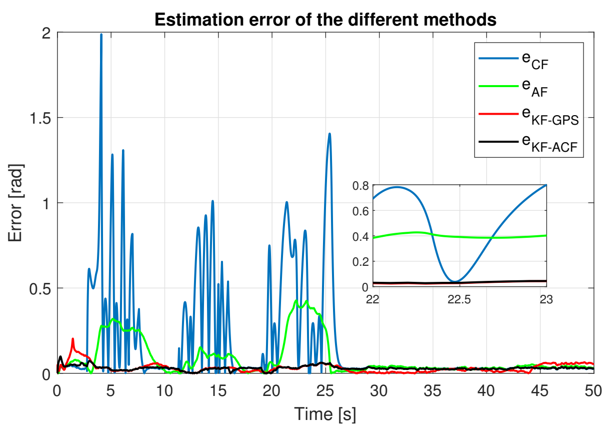

Fig. 13: Estimation error of the CF, AF, KF-GPS and KF-ACF

Together, the figures show the advantage of an extra estimation based on the Kalman Filter over solely an adaptive law or a fixed gain.

VI. CONCLUSIONS

The problem of magnetic field distortion which leads to errors in ψ-estimation has been solved by implementing and redesigning the Adaptive Filter (AF). Hereby, an LTV Kalman Filter has been used as the main estimator where we have extended the method for Quadcopters. An extensive observability analysis has been performed in which a metric has been defined and tested for the Degree of Observability of the system. The adaptation and estimation scheme proposed in this thesis was proven to be effective. The RMSE of the proposed KF-ACF has an improvement of a factor 4.5 over the Adaptive Filter (AF) and an improvement of a factor 11.5 over the conventional Complementary Filter (CF).

VII. FUTURE WORK

Future work will include the testing of filters in an experimental setup and validation of the filters on a real system. A next step which would improve the work would be to analyze stability of the adaptive filters.

The adaptive ECF method as proposed can be validated first by simulations and then by experiments. The current extension of the ECF describes an adaptive logic based on metrics which handle disturbances in vector measurements. However, we believe that the addition of another measurement, the KF-GPS, can improve the overall performance of the ECF. To do this, measurements in $\{I\}$ have to be added to measurements in $\{B\}$. In literature many other estimation methods can be considered to improve the adaptation and estimation filter such as particle filtering or Extended Kalman Filtering.

REFERENCES

[1] J. Callmer, D. TÃűrnqvist, and F. Gustafsson. Robust heading estimation indoors using convex optimization. pages 1173–1179, July 2013.

[2] Nagesh Yadav and Chris J. Bleakley. Accurate orientation estimation using ahrs under conditions of magnetic distortion. 2014.

[3] V. Renaudin, M. H. Afzal, and G. Lachapelle. New method for magnetometers based orientation estimation. pages 348–356, May 2010.

[4] Harro Ranter. Asn aircraft accident boeing 737-241 pp-vmk s, Sep 1989.

[5] IvÃạn F. MondragÃşn, Pascual Campoy, Carol Martinez, and Miguel Olivares. Omnidirectional vision applied to unmanned aerial vehicles (uavs) attitude and heading estimation. *Robotics and Autonomous Systems*, 58(6):809âĂŞ819, 2010.

[6] G. AraguÃąs, C. Paz, D. Gaydou, and G. P. Paina. Orientation estimation fusing a downward looking camera and inertial sensors for a hovering uav. pages 1–6, Nov 2013.

[7] L. Meier, P. Tanskanen, F. Fraundorfer, and M. Pollefeys. Pixhawk: A system for autonomous flight using onboard computer vision. pages 2992–2997, May 2011.

[8] Inkyu Su and Peter Corke. 100hz onboard vision for quadrotor state estimation. *Proceedings of Australasian Conference on Robotics and Automation, 3-5 Dec 2012, Victoria University of Wellington, New Zealand.*

[9] Abd El Rahman Shabayek, Cédric Demonceaux, Olivier Morel, and David Fofi. Vision based uav attitude estimation: Progress and insights. *Journal of Intelligent & Robotic Systems*, 65(1):295–308, Jan 2012.

[10] Muhammad Afzal, ValÃľrie Renaudin, and GÃľrard Lachapelle. Assessment of indoor magnetic field anomalies using multiple magnetometers. pages 525–533, 01 2010.

[11] Bingfei Fan, Qingguo Li, and Tao Liu. How magnetic disturbance influences the attitude and heading in magnetic and inertial sensor-based orientation estimation. *Sensors*, 18(2):76, 2017.

[12] R. Mahony, T. Hamel, and J. Pflimlin. Nonlinear complementary filters on the special orthogonal group. *IEEE Transactions on Automatic Control*, 53(5):1203–1218, June 2008.

[13] A. R. P. AndriÃńn, D. Antunes, M. J. G. v. d. Molengraft, and W. P. M. H. Heemels. Similarity-based adaptive complementary filter for imu fusion. pages 3044–3049, June 2018.

[14] Han-Fu Chen. On stochastic observability and controllability. *Automatica*, 16(2):179 – 190, 1980.

[15] R. Mahony, V. Kumar, and P. Corke. Multirotor aerial vehicles: Modeling, estimation, and control of quadrotor. *IEEE Robotics Automation Magazine*, 19(3):20–32, Sept 2012.

[16] Dave Kooijman, Duarte Antunes, and Angela P Schoellig. Quadrotor trajectory tracking using cascaded model predictive control and tracking control in s2 x s1. 2018.

[17] Vibhor L. Bageshwar, Demoz Gebre-Egziabher, William L. Garrard, and Tryphon T. Georgiou. Stochastic observability test for discrete-time kalman filters. *Journal of Guidance, Control, and Dynamics*, 32(4):1356âĂŞ1370, 2009.

[18] Daniel Viegas, Pedro Batista, Paulo Oliveira, and Carlos Silvestre. On the stability of the continuous-time kalman filter subject to exponentially decaying perturbations. *Systems Control Letters*, 89:41âĂŞ46, 2016.

[19] Andrew Whalen, Sean Brennan, Timothy D. Sauer, and Steven J. Schiff. Observability and controllability of nonlinear networks: The role of symmetry. *Physical Review X*, 5, 01 2015.

[20] L. A. Aguirre. Controllability and observability of linear systems: some noninvariant aspects. *IEEE Transactions on Education*, 38(1):33–39, Feb 1995.

[21] Jinyan Ma, Quanbo Ge, and Teng Shao. Impact analysis between observable degrees and estimation accuracy of kalman filtering. pages 124–128, Jan 2015.

[22] Marcin Witczak, VicenÃğ Puig, Damiano Rotondo, and Piotr Witczak. A necessary and sufficient condition for total observability of discrete-time linear time-varying systems. *IFAC-PapersOnLine*, 50(1):729 – 734, 2017. 20th IFAC World Congress.

[23] M. He, Q. Ge, J. Ma, and T. Chen. Observable degree analysis of kalman filter with correlated noises. pages 517–522, Aug 2017.

Technische Universiteit
Eindhoven
University of Technology

Declaration concerning the TU/e Code of Scientific Conduct for the Master's thesis

I have read the TU/e Code of Scientific Conduct[i].

I hereby declare that my Master's thesis has been carried out in accordance with the rules of the TU/e Code of Scientific Conduct

Date

........04 - 10 - 2019..

Name

........Hasan Elisu..

ID-number

........0852221..

Signature

....

Submit the signed declaration to the student administration of your department.

[i] See: http://www.tue.nl/en/university/about-the-university/integrity/scientific-integrity/
The Netherlands Code of Conduct for Academic Practice of the VSNU can be found here also.
More information about scientific integrity is published on the websites of TU/e and VSNU